ISSN 1063-7729, Astronomy Reports, 2011, Vol. 55, No. 10, pp. 918–927. © Pleiades Publishing, Ltd., 2011.
Original Russian Text © M.A. Livshits, A.M. Urnov, F.F.Goryaev, L.K. Kashapova, T.I. Kal'tman, 2011, published in Astronomicheskii Zhurnal, 2011, Vol. 88, No. 10, pp. 997–1007.

Physics of Post-Eruptive Solar Arcades: Interpretation of RATAN-600 and STEREO Spacecraft Observations

M. A. Livshits[1*], A. M. Urnov[†2], F. F. Goryaev[2,3], L. K. Kashapova[4], I. Yu. Grigor'eva[5], and T. I. Kal'tman[6]

[1] *Institute of Terrestrial Magnetism, Ionosphere, and Radio Wave Propagation, Russian Academy of Sciences, Troitsk, Moscow oblast', 142190 Russia*

[2] *Lebedev Physical Institute, Russian Academy of Sciences, Leninskiĭ pr. 53, Moscow, 119991 Russia*

[3] *Royal Observatory of Belgium, Avenue Circulaire 3, 1180 Brussels, Belgium*

[4] *Institute of Solar-Terrestrial Physics, Siberian Division of the Russian Academy of Sciences, P.O. Box 4026, Irkutsk, 664033 Russia*

[5] *Main Astronomical Observatory, Russian Academy of Sciences, Pulkovo, St. Petersburg, 196140 Russia*

[6] *St. Petersburg Branch of the Special Astrophysical Observatory, Russian Academy of Sciences, Pulkovo, St. Petersburg, 196140 Russia*

Received December 14, 2010; in final form, December 27, 2010

Abstract—Results of simultaneous measurements of radiation fluxes from post-eruption arcades on the Sun at 171, 195, 284, and 304 Å (from STEREO spacecraft data) and at radio wavelengths (from the RATAN-600 radio telescope) are presented. An original probabilistic approach developed earlier by Urnov was used to determine the differential emission measure. This method requires no regularization, and the obtained results do not depend on the choice of the temperature grid. This approach has yielded the differential measure of emission at temperatures approximately from 0.3 to 15 MK. The subsequent calculation of thermal magnetobremsstrahlung in a multi-temperature model with the magnetic field decreasing with height produces a spectrum similar to that observed on RATAN-600. Thus, in many non-stationary events with modest powers, a thermal multi-temperature model is quite able to explain the emission of post-eruption arcade systems, and it is not necessary to invoke the emission of accelerated particles. The proposed model enables direct estimation of the ratio of the magnetic and gas pressures at the tops of post-eruption arcades, and determination of the conditions required for the origin of secondary nonstationary processes in the decay stage of the main flare.

DOI: 10.1134/S1063772911100064

1. INTRODUCTION

One distinctive feature of solar flares is the formation and subsequent evolution of loops filled with hot plasma. As a rule, the first loops appear in images of X-ray or vacuum UV (VUV) lines near the source of impulsive energy release, after with the system of loops quickly propagates along a neutral line of the magnetic field. In somewhat powerful processes (C, M, and X class flares), some groups of loops integrated into one large-scale system in the final stage of the event often develop sequentially.

As is known, post-eruption (PE) arcades were observed earlier in chromospheric lines, most frequently in the Hα line. They appeared after the flare maximum, and their height gradually increased, reaching approximately 30 000 km. In very rare cases, the escape of a PE arcade into interplanetary space (so-called dynamic flares, Švestka) was observed. The life times of arcades are from several hours to several days. In the last solar cycle, arcades were regularly observed by the SOHO spacecraft in several VUV ranges, most notably at 195 Å. The SOHO observations covered temperatures from 0.1 to 3.0 MK. The detection by the KORONAS-F satellite of long-lived structures in the 8.42-Å line of the MgXII ion [1], testifying to the presence of large plasma structures with still higher temperatures of 6–15 MK was an important discovery. Due to their shape, these sources were called "spiders." They either coincide with PE arcades or are immediately adjacent to their tops.

[†] Deceased.
[*] E-mail: maliv@mail.ru

Physically, the prolonged existence of hot plasma in the decay stage of flares is due to prolonged heating, which compensates small radiative energy losses. Evidence for continuous energy release after the impulsive phase was obtained, e.g., by the Nobeyama (17 GHz) and SSRT (5.7 GHz) radioheliographs for the powerful limb flare of November 2, 1992 [2]. Among numerous recent studies, we also note [3], which initiated the study of a cool and hot PE arcade using its emission in soft and hard X-rays. The plasma-cooling timescales in PE loops for temperatures from about 4×10^6 to 10^4 K were estimated in [4].

The flare of November 2, 1992 was also considered in [5] using simultaneous observations in soft X-rays and the Hα line. It was supposed in [5] that the gas pressure approaches the magnetic pressure near the loop tops, as was concluded based on KORONAS-F data by Grechnev et al. [6]. This same paper lists the main references on the determination of physical conditions in PE arcades.

Physical conditions in the plasma inside the arcades, especially at the beginning of their lifetimes, depend on processes at the onset of a flare. Here, the main factor is the efficiency of particle acceleration and the degree of particle confinement in the magnetosphere of the active region. Beams of accelerated particles penetrating into dense atmospheric layers near the loop bases result in explosive evaporation, and hot plasma fills coronal loops. Of course, the effect of accelerated particles on the state of the plasma in arcades decreases with time, if no repeated acts of impulsive energy release occur. Until now, it has been assumed that accelerated particles make a significant contribution to the radio and X-ray emission of PE arcades, especially in the initial stages of their lives.

Since the 1980s, RATAN-600 data have also been applied to the interpretation of long-lived events, such as the flare of September 22, 1980 [7]. In total, about ten PE arcades (either developing at the limb or projected onto the disk) have been studied in more or less detail using radio data. Virtually all cases encountered the same difficulties in logical interpretation, described in most detail in [8], which was dedicated to a PE arcade that developed after the postlimb flare of January 25, 2007. This paper presents observations obtained on the RATAN-600 only half an hour after the maximum of a C6.3 flare. The spectral evolution of the radio emission source was quite unusual: at the beginning, the 1.8–5.0-cm spectrum was flat, after which the flux appreciably decreased toward short wavelengths. A flat radio spectrum is usually attributed to thermal emission of an optically thin, isothermal source. Therefore, the RATAN-600 observations suggested that a large amount of hot plasma should be involved in the formation of the arches. On the other hand, the spectrum fell off toward short wavelengths during the decay of the event, which is characteristic of magnetobremsstrahlung of accelerated particles. This contradicted observations at meter wavelengths (Institute of Terrestrial Magnetism, Ionosphere, and Radiowave Propagation, experiment WIND/Wave), which did not provide any evidence for nonthermal effects at that time.

We have used available observations from the STEREO spacecraft to find a possible solution of this inconsistency, using the event of January 25, 2007 as an example. We have determined the amounts of plasma having various temperatures and recalculated the thermal magnetobremsstrahlung spectrum. The conclusion of this paper summarizes our results and discusses some problems of the physics of PE arcades.

2. RATAN-600 OBSERVATIONS

Regular multi-wavelength observations of the Sun on the RATAN-600 telescope [9] have been carried out since November 1974. In most cases, these are observations at the meridian, during the transit of the Sun across the fixed telescope beam. Our recent observations use an antenna system consisting of the Southern Sector of the antenna and a flat periscope mirror (S+P). This allows us to obtain from a few to 61 strip scans per day. We can determine the position of a source on or beyond the solar disk, as well as its radiation flux, angular size, and degree of circular polarization fairly accurately. We carefully isolated the source above the emission level of the quiet Sun in the central part of the solar disk and near the limb, taking into account and eliminating spurious signals in the polarization channel. The half-power beamwidth of the S+P antenna system is $17'' \times 13'$ at 15 GHz.

On January 25, 2007, during RATAN-600 observations of the Sun at 6–16 GHz at seven azimuths with an interval of 35 min, we detected radio emission from a developing PE arcade in an active event at the eastern limb, which consisted of a large-scale coronal mass ejection (CME) and an associated C6.3 flare behind the eastern limb. The flare began at 06:33 UT, with the bases of the coronal loops being behind the limb. A radio source (Fig. 1) was observed above the eastern limb during 3.5 h. The maximum of its emission was projected against the top of a forming arcade observed at 195 Å by SOHO/EIT and STEREO. A RHESSI coronal source of X-ray radiation at energies above 12 keV was located at approximately the same place.

The maximum intensity of the radio emission was projected against the tops of the arcades. The arcade developed in the south approximately until 9 h, when

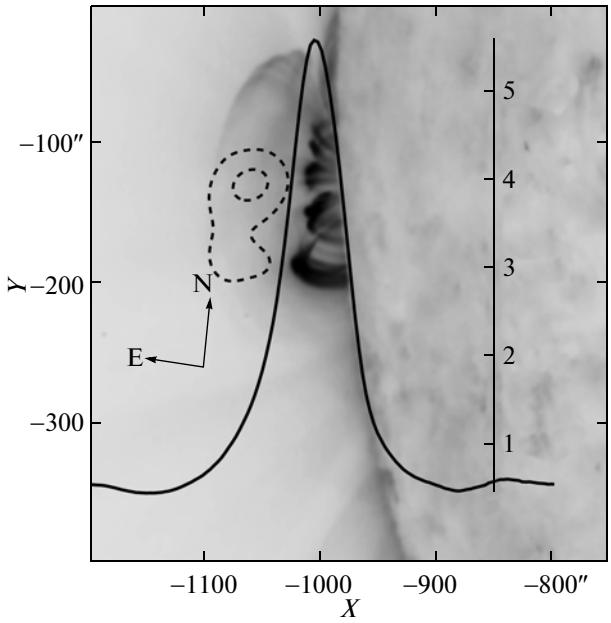

Fig. 1. Position of the 6–12-keV X-ray source (RHESSI; contours are at 90 and 60% of the maximum) and source scan at 10.33 GHz (RATAN-600) relative to the arcade observed at 195 Å (SOHO). All observations were carried out at 08:18 UT. The coordinates are measured from the solar center. The vertical scale shown in the right-hand part of the graph corresponds to the excess of the brightness temperature of the source above the level of the quiet Sun in units of 10^4 K.

its northern part began to emerge. In the RATAN-600 observations, the radio emission from the northern (new) loop system became appreciable starting at 09:26 UT, as a second maximum in radio scans of the source above the limb [8, Fig. 2h]; by the end of the observations, it was stronger than the radio source associated with the arch system that formed first. At the same time, the radio emission of the old loop system was polarized more strongly (the degree of circular polarization was about 12%).

Let us consider the integrated characteristics of the radio source above the limb (associated with the entire PE arcade) and their evolution during the formation of the arcade. The effective size D of the radiating region along the scanning direction was determined as $D = (A^2 - B^2)^{1/2}$, where A and B are the source size at the scan mid-elevation and at the RATAN-600 half-power beamwidth, respectively. It was assumed that the brightness strip-distribution over the entire source and the beam are close to Gaussian. The effective sizes of the radio source at all frequencies throughout the range 6–16 GHz turned out to be virtually identical. In the first observation, the effective size of the radiating radio region is larger than the small loop in the 195-Å line (SOHO/EIT) at the solar limb. In late observations, the radio size is approximately the same as the projection of the entire loop system on the scanning direction. The value of D was about 1 arcmin, and increased somewhat during 3 h of the observations.

The radio intensity was high right after the flare maximum at the beginning of the formation of the PE arcade, after which it decreased appreciably. The character of the spectrum of the total radio flux of the arcade changed with time. Figure 2 shows the evolution of the total flux spectrum for the radio source above the limb associated with the PE arcade. The spectra are plotted as an upper envelope using all frequencies in the range used. The flux measurement errors (10–15%) were determined by the accuracy of the source selection, as well as by the calibration. We used RATAN-600 data for the Moon and Crab Nebula for the absolute flux calibration, also taking into account integrated fluxes of the Sun obtained by the Radio Solar Telescope Net (RSTN). For this event, we used observations of the Learmonth Station (Australia). All measured fluxes are in solar flux units ($1\ \mathrm{sfu} = 10^{-22}\ \mathrm{W\ cm^{-2}Hz^{-1}}$).

The total-flux spectrum of the radio source in early stages of formation of the PE arcade is essentially flat. This suggests that thermal emission dominates just after the flare maximum.

Considering thermal bremsstrahlung of optically thin, hot plasma as the dominant mechanism for the radio emission in early stages of formation of an arcade, we can estimate the emission measure EM using the well-known expression

$$S\,[\mathrm{sfu}] \sim 3 \times 10^{-45} \mathrm{EM}[\mathrm{cm}^{-3}](T[\mathrm{K}])^{-1/2},$$

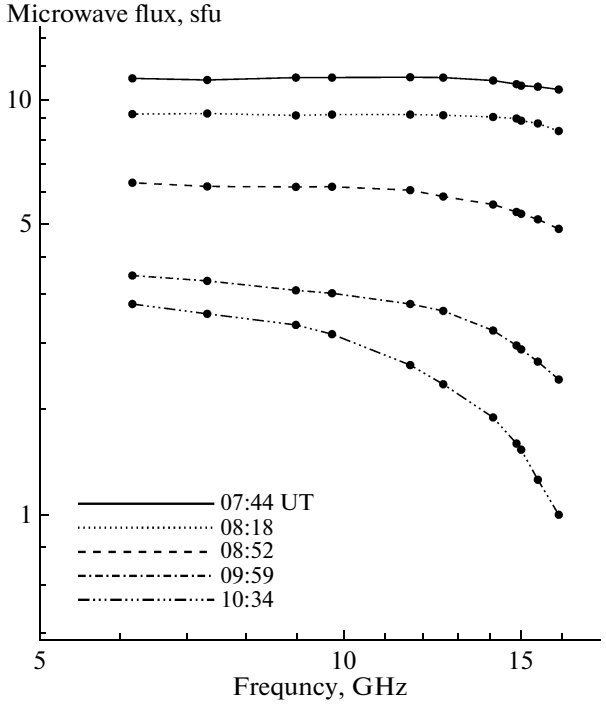

Fig. 2. Evolution of the radio spectrum for the event of January 25, 2007 (RATAN-600).

where S is the total radio flux and T the temperature of the radiating plasma.

Using the flux S at the highest frequency (16.7 GHz) and assuming that the brightness temperature T_b at the lowest frequency (6 GHz) provides a lower limit for the kinetic temperature of the plasma in the arcade (optical depth $\tau(6\ \mathrm{GHz}) \gg \tau(16.7\ \mathrm{GHz})$), we obtain $T_b = 5.2$ MK, $\mathrm{EM} = 14.6 \times 10^{48}$ cm^{-3} at 07:44 UT and $T_b = 2.4$ MK, $\mathrm{EM} = 7.5 \times 10^{48}$ cm^{-3} at 08:18 UT.

Assuming that the volume of the radiating region is $V = D^3$, where D is the effective size of the radio source, we obtain mean electron densities of 2.2×10^{10} and 1.0×10^{10} cm^{-3}, respectively. Note that the radio spectra of the PE arcade obtained 3 h after the flare maximum in the event of January 25, 2007 essentially coincide with the RATAN-600 spectra for the PE arcade at late stages of the eruptive event of October 22, 2001, 6–8 h after the maximum of a class M flare [1, 6]. Of course, the emission measure and density at 07:44 UT could be overestimated (by a factor of two for the density), since not all the radiation flux during the formation of an arcade is thermal.

3. RESULTS OF THE STEREO OBSERVATIONS

In addition to the SOHO data, we considered observations of the event of January 25, 2007 from one of the coronagraphs of the STEREO-B spacecraft. This enabled us to carry out an analysis at a higher imaging rate, with better knowledge of the VUV bands, and with a more reliable data calibration.

The Solar TErrestrial RElations Observatory (STEREO) is comprised of two identical spacecraft launched on October 26, 2006. The equipment of both spacecraft include four instrument packages for the analysis of the outer atmosphere of the Sun and interplanetary space out to the Earth's orbit. We used data from the Extreme UltraViolet Imager (EUVI) in the SECCHI (Sun Earth Connection Coronal and Heliospheric Investigation) package. Its design is similar to EIT (SOHO), with an additional facility for an image shift of up to 7″ (as for TRACE). The radius of the field of view is 1.7 solar radii, and the pixel size is 1.6″. The images of the Sun are recorded in four VUV bands: 171 Å (FeIX, FeX), 195 Å (FeXII, FeXXIV), 284 Å (FeXV), and 304 Å (HeII). The exposures were from 2 to 32 s with imaging intervals from 2.5 to 32 min. More details can be found in [10].

For this event, we used observations obtained on one of the spacecraft, STEREO Behind (event N17 in the catalog of flares and CMEs [11]). At that time, the difference in the angles of view of the two spacecraft (Ahead, Behind) was only 0.5°. Therefore, we could assume that the event was observed from the same directions as at ground-based observations.

We chose a 1.4×10^{20} cm^2 area in the image of the entire Sun in each of the four bands (Fig. 3, contour),

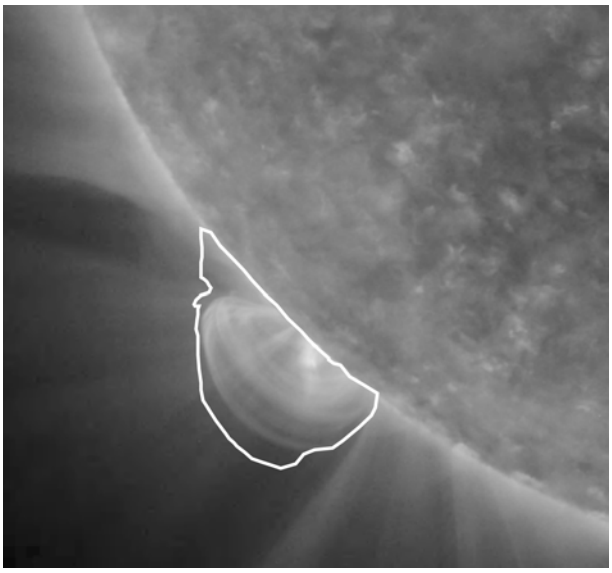

Fig. 3. STEREO 171-Å image (07:40 UT). The contour delimits the area from which radiation fluxes were measured. The original STEREO-B image is shown; its orientation differs from the standard one. The frame size is 650″ × 650″.

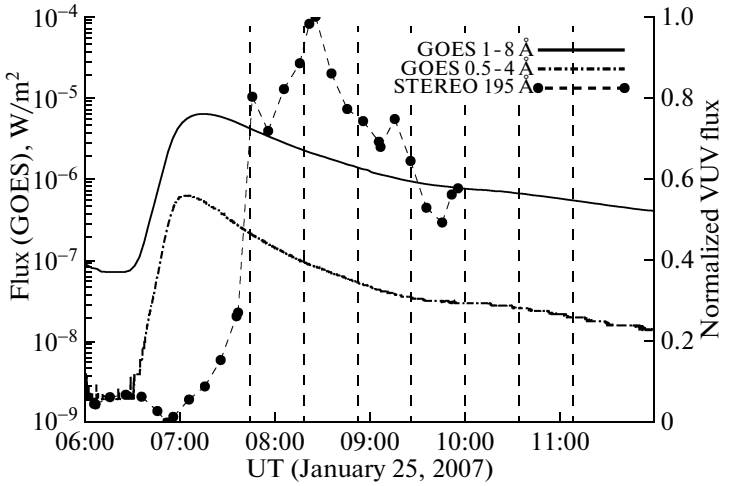

Fig. 4. Time profiles of the total flux of the Sun in soft X-rays and the VUV. The vertical dashed lines show the times of the RATAN-600 observations.

which delimited the arcade in the VUV at all times of the RATAN-600 observations. It is important that all of the area was above the solar limb. Otherwise, the difference between the brightnesses of the disk and of the overlying coronal layers, particularly in the 304-Å line, strongly hampers the analysis. The radiation fluxes of the EUVI-coronagraph B with the background subtracted were summed over all pixels in the selected area. Figure 4 shows the variation of the radiation fluxes at 195 Å (the most frequently observed band), together with the GOES records, with the times of the RATAN-600 scans indicated. Note also that the X-ray maximum at about 7 UT in the GOES and RHESSI ranges with energies from 3 to 50 keV [8, Fig. 6a] was completely absent in the VUV (STEREO). In the event of January 25, 2007, the loop feet were behind the limb, and the emission of the coronal source (of accelerated particles and high-temperature plasma) was virtually invisible in the VUV. The first RATAN-600 observation, obtained approximately 30 min after the flare maximum, coincided with the beginning of the recording of the arcade emission in the VUV (see also the evolution of the 171-Å in [11]).

Thus, the STEREO and RATAN-600 observations reflect the development of the PE arcade. Note

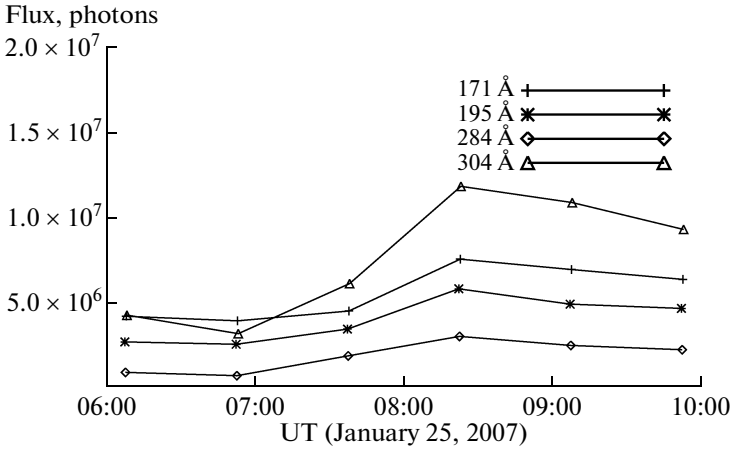

Fig. 5. Time dependence of the fluxes in four VUV ranges (EUVI/SECCHI) for the region shown in Fig. 3.

that the main maximum at 195-Å (about 08:30 UT in Fig. 4) is related to the appearance in the field of view of the second (northern) part of the arcade.

We selected data for common times from 06–10 UT and measured the radiation fluxes in all four EUVI (SECCHI) ranges (the number of photons recorded from the chosen area). Figure 5 presents the time variation of the fluxes. We used these data as a base for constructing a multi-temperature model of the source, described below.

4. DIFFERENTIAL EMISSION MEASURE (DEM)

The radiation flux in spectral channel L emitted in a wavelength intreval $\Delta\lambda(L)$ from an optically thin plasma source of volume V is

$$I_L = \int\limits_V G\left(L, T(\mathbf{r})\right) N_e^2(\mathbf{r}) d\mathbf{r}, \qquad (1)$$

where $T(\mathbf{r})$ and $N_e(\mathbf{r})$ are the spatial distributions of the temperatures and integrated electron densities in the volume V, and $G(L,T)$ is the temperature-response function in the channel L, determined from the spectral luminosity function $\widetilde{F}(\lambda; T, N_e)$, which, in turn, is calculated for a particular model for the radiating plasma (including the condition for the coronal approximation and the condition for an optically thin plasma) and is integrated over the wavelength interval $\Delta\lambda(L)$ with the instrument function of the spectral device $f(L,\lambda)$ for channel L:

$$G(L,T) = \frac{1}{N_e^2} \int\limits_{\Delta(L)} f(L,\lambda)\widetilde{F}(\lambda; T, N_e) d\lambda. \qquad (2)$$

Using the concept of the differential emission measure (DEM) describing the temperature structure of the radiating plasma, the measured quantity I_L can be written as an integral over the temperature:

$$I_L = \int\limits_{\Delta T} G(L,T) y(T) dT, \qquad (3)$$

where $y(T)$ is the temperature distribution of the DEM.

The problem of finding the distribution $y(T)$ is stated as the inverse problem of spectroscopy, and reduces to solving a system of integral equations of the form (3) for the available set of spectral channels $\{L_i\}$ (i is the channel number). We reconstructed the temperature profile of the DEM over the STEREO channels using the Bayes Iteration Method (BIM), developed in a probabilistic approach and based on Bayes' theorem [12, 13]. In this probabilistic approach, which we used to mathematically formalize the inverse problem of spectroscopy, formula (3) is replaced by the formula for the total probability

$$P(L) = \int\limits_{\Delta T} P(L|T) P(T) dT \qquad (4)$$

for the probabilistic distributions $P(L)$, $P(L|T)$, and $P(T)$, which are positively defined and obey the normalization condition

$$\sum_L P(L) = 1, \quad \sum_L P(L|T) = 1, \qquad (5)$$

$$\int\limits_{\Delta T} P(T) dT = 1,$$

where the summation and integration are carried out over all spectral channels and over the given temperature range, respectively. These distributions are interpreted as probability densities of the random variables L and T, defined on corresponding sets of complete

systems of events: $P(T)$ is the probability density for a photon to be emitted by plasma at temperature T, $P(L)$ is the probability for a radiated photon to be detected in channel L, and $P(L|T)$ is the conditional probability for the event L under the condition T.

We applied the BIM scheme [12] to find the unknown function $P(T)$:

$$P^{(n+1)}(T) = P^{(n)}(T) \sum_L \frac{P^{\exp}(L)}{P^{(n)}(L)} P(L|T), \quad (6)$$

where $P^{\exp}(L) = I_L^{\exp} / \sum_{L'} I_{L'}^{\exp}$ is the observed probability distribution in channels $\{L_i\}$, and the $P^{(n)}(L)$ are calculated using (4) with the nth approximation $P^{(n)}(T)$. In (6), the left-hand side $P^{(n+1)}(L)$ is interpreted as an estimate for the nth hypothesis of the distribution $P(T)$; $P^{\exp}(L)/P^{(n)}(L)$ and the χ^2 criterion are used to assess the agreement between the calculated and observed fluxes and to control the convergence of the iterative procedure. We used an equiprobable distribution as the zeroth approximation, $P^{(0)}(T)$. Using the obtained solution for $P(T)$, we calculated the distribution $y(T)$ for the DEM:

$$y(T) = \frac{P(T) \sum_L I_L^{\exp}}{\sum_L G(L,T)}. \quad (7)$$

In the DEM calculations, we used the temperature responses $G(L,T)$ for the STEREO channels calculated by the CHIANTI package and taken from the corresponding solar software (solarsoft for SOHO/STEREO). These functions are shown in Fig. 6, which show the temperature regions of formation of the emission for the corresponding spectral channels. The results of the calculations of the DEM temperature profiles as functions of the logarithm of the temperature (in Kelvin) from the STEREO data for regions with PE arcades are presented in Fig. 7.

The obtained distributions $y(T)$ for the DEM can be compared with the data derived from X-ray observations. The X-ray spectra for times close to the RATAN-600 scans were constructed using the RHESSI data. Two spectra were presented earlier [8, Fig. 6a]. The analysis of these spectra demonstrates that the thermal part of the emission at 1–10-keV slowly decreases after 08:18 UT, associated with a small change in temperature $T \sim 13.3$ MK and a considerable decrease in the emission measure (EM). In the model chosen by us, EM $= 1.3 \times 10^{48}$ cm^{-3}. This EM is only slightly lower than the value following from the above analysis of the VUV observations of the high-temperature region. There, the changes in the DEM integrated over all regions with $T = 5$–8 MK appreciably exceed the value found from the soft X-ray spectrum. Given that there is some difference in the temperatures, we consider the agreement of these conclusions to be good.

We adopt for the PE arcade as a whole EM$= 4 \times 10^{48}$ cm^{-3}. Various simple estimates taking into account the small hydrostatic decrease of the density with height result in a mean density in the loops close to 0.5×10^9 cm^{-3}, or, allowing for the filling factor, $(0.5$–$1.0) \times 10^{10}$ cm^{-3}. These latter values coincides with the estimate of Grechnev et al. [6]. This reflects the fact that, when the energies of the entire nonstationary processes are comparable, the density varies little in different PE arcades, or in the course of a particular event.

5. RATAN-600 RADIO SPECTRA AND THEIR INTERPRETATION

During this work, the hypothesis arose that the unusual nature of the RATAN-600 spectra, especially after the disappearance of obvious nonthermal phenomena, was related not to the effect of accelerated particles but to the need to take into account regions with different temperatures. The relevant data were obtained above, and the values DEM(T) for the PE arcade (Fig. 7b) can be used to model the source. A substantial difficulty is assigning heights to regions of plasma with different temperatures, which cannot be done without invoking additional observations or assumptions. Calculations of magnetobremsstrahlung for a system of loops that fully incorporate determinations of DEM(T) still lie in the future. Below, we propose a simple model illustrating the "multitemperature" effect of the emission source.

Since the late 1960s, magnetobremsstrahlung has been successfully applied to interpret data on the radio emission of sources above sunspots [14–17]. An important factor here was that, above the sunspot umbra, the transition from cool to hot (coronal) layers takes place simultaneously with a decrease in the magnetic-field intensity from thousands to tens of Oersted. In contrast to a vertical tube, a model for loops in active regions was recently developed, with thermal magnetobremsstrahlung of a hot loop in the form of a torus with constant magnetic intensity at its axis. One peculiarity of this model is its unusual surface of gyroresonant levels [18, 19] (with more detailed account for chromospheric layers [20]). The existence of very long loops connecting points with opposite field polarity in the active corona justifies the assumption that the field in them is constant. The PE arcade is located right above the neutral line of the (longitudinal) magnetic field, and the distance between the bases of the loops does not considerably exceed their height, which reaches 30 000 km. The magnetic fields at the bases of some arches located near sunspots can reach values of about 1000 Oe.

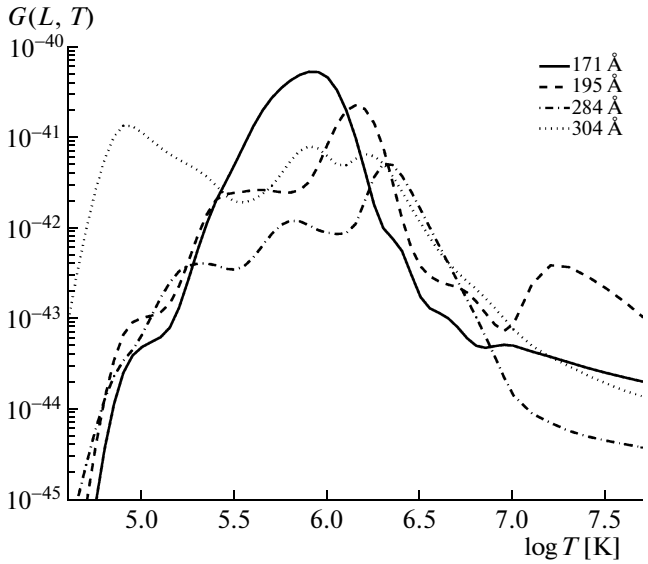

Fig. 6. Contribution functions for EUVI channels of the STEREO spacecraft.

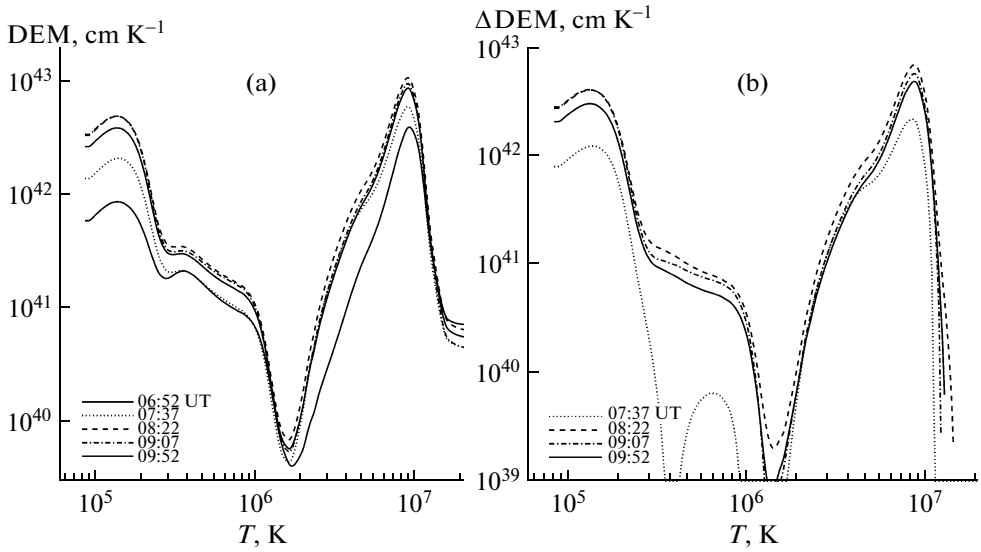

Fig. 7. (a) Distribution DEM(T) for different times. (b) Difference $\Delta\mathrm{DEM}(T,t) = \mathrm{DEM}(T,t) - \mathrm{DEM}(T,t_0)$ for these times and for the initial time 06:52 UT (in Fig. 7a, the curve for this initial time is the lowest one).

At the tops of these arches, the fields are one to two orders of magnitude weaker. Therefore, the radio emission arises predominantly near the loop bases. Note, however, that the rate of decrease of the field with height in the lower parts of arches can be lower than above a sunspot umbra.

As an example, Fig. 8 presents a calculation of magnetobremsstrahlung for two large vertical tubes observed at an angle of 45° to the axis. Proceeding from the analysis of DEM(T), we assume that the temperature in the first is $T = 4$ MK, and in the second $T = 8$ MK. Here, we neglect the existence of gas with temperatures about 0.1 MK, since these regions make a negligible contribution to the thermal magnetobremsstrahlung of the arcade. We assume that the height distribution of the density in the cool and hot "loop" follows a hydrostatic law, with the density at their bases $n_0 = 5 \times 10^{10}$ cm^{-3} and with the scale heights 1.4×10^{10} and 2.8×10^{10} cm, respectively (when choosing these dependences, we took into account results obtained in soft X-rays). We assumed a loop radius of 5000 km. We present here the results of these calculations for a vertical magnetic field $H(h) = H_0(1 - h/h_0)$, with $H_0 = 1000$ Oe

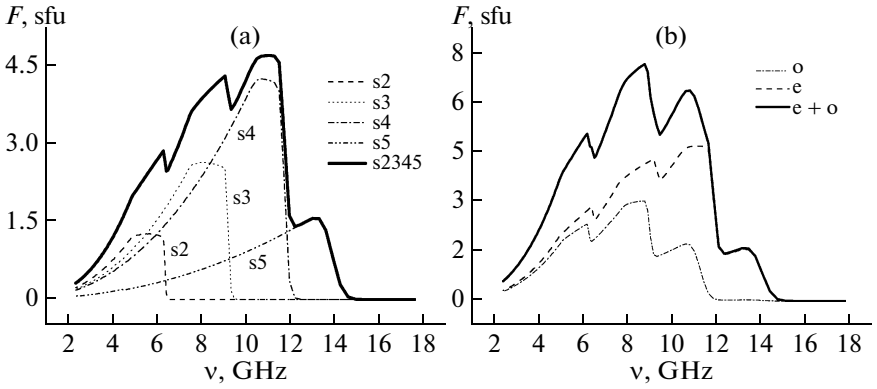

Fig. 8. (a) Magnetobremsstrahlung of a column of hot plasma. The harmonics 2–5 of the extraordinary wave and their sum are presented. (b) Emission of cool and hot columns of plasma in the ordinary (lower curve) and extraordinary (middle curve) emission. Upper curve: total emission.

and $h_0 = 70\,000$ km, though the calculations were also carried out for $H_0 = 700$ Oe and $H_0 = 2000$ Oe. Note also that the plasma columns do not screen each other, and there is no surrounding plasma.

As a result of the calculations, we found that the 2–15 cm (15–2 GHz, see Fig. 8a) emission comes from flat gyrolevels of harmonics 2–5 (typical harmonics for sunspots are 2 and 3). In particular, the emission of the 2nd harmonic appears at 4–13 cm, with a maximum at 6 cm. The emission at the 3rd harmonics at 6 cm is only slightly weaker than the emission at the 2nd harmonic, and peaks at 4 cm. The maximum contribution at 3 cm is made by the 4th harmonic, and the maximum contribution at 2.1 cm by the 5th harmonic.

The sum of the emission of the gyrofrequency harmonics 2–5 is shown in Fig. 8b. First, the estimates demonstrate that the emission fluxes exceed the thermal emission of the corresponding sources in the absence of the magnetic field. This testifies to appreciable efficiency of the magnetobremsstrahlung mechanism. Second, excess emission appears in the required range, 6–16 GHz, with a fairly similar spectrum. The sharp cutoff of the spectrum of polarized emission at high frequencies is due to the adopted model for the magnetic field. In the method proposed by G.B. Gelfreikh (the method is described in [21]), the magnetic field was determined using precisely this feature. This flux decrease toward high frequencies is not so prominent for a system of multiple loops.

A difficulty arises in the considered simple model for two vertical columns: the degree of polarization turns out to be higher than the observed values. However, this should be expected. The actual system includes more than ten loops with slightly different physical conditions and angles of inclination relative to the observer. Of course, these factors result in an appreciable decrease in the degree of polarization.

Preliminary calculations taking into account the total emission of the entire region occupied by the loops (the emission of the loops with the field and of the environment free of an appreciable field) demonstrate that it is possible to obtain radio spectra of PE arcades similar to those observed on the RATAN-600. This model already incorporates all the information on the DEM(T) distribution and a more realistic form of the loops. However, the main difficulty is the uncertainty in the choice of the magnetic-field distribution in a loop at different heights.

6. CONCLUSIONS

Powerful nonstationary processes on the Sun include CMEs and the formation of loops filled with dense hot plasma. A PE arcade is the most frequent result of the evolution of flare loops, though it sometimes appears along a neutral line of the magnetic field at a large distance from the center of the flare. Numerical modeling and analytical methods applied to processes inside arches lead to similar results: very modest heating of plasma, e.g., at the top of the loops, is sufficient for the arcade to exist during the entire time this source of energy operates. It is necessary to compensate radiative losses, which are minimal at plasma temperatures of about 5 MK. Unfortunately, there remain many questions (about the origins of PE arcades, determination of their heights, the filling of the loops with material, etc.), partially connected with particulars of the developing MHD process. These problems are still far from being solved.

Modern observations provide a powerful impetus to studies of the physics of PE arcades. For instance, it is now possible to determine to sufficient accuracy the temperatures and densities at the tops of arches. Applying some assumptions about the magnetic field in the corona, Grechnev et al. [6] concluded that the

gas and magnetic pressures at the loop tops were approximately equal. When the magnetic "beta" value approaches unity, gas-dynamic effects begin to dominate. This may determine the height to which the loops rise, as well as the conditions for the ejection of plasma into interplanetary space in the decay stages of nonstationary processes on the Sun.

Long-term observations of PE arcades with the RATAN-600 have revealed unusual behavior of the radio spectrum: just after the formation of an arcade, the spectrum is flat at 6–16 GHz, and then decreases with time toward high frequencies. In addition, the intensity, e.g., at frequencies about 6 GHz (5 cm) decreases already after the formation of an arcade. This testifies to attenuation of the emission measure of the main source of thermal plasma emission. However, in this case, the sloped spectrum testified to magnetobremsstrahlung of accelerated particles, as was believed earlier.

Carrying out a modern analysis of the STEREO data has enabled us to resolve the contradiction between the presumed thermal emission for an isothermal source and the form of the spectra, characteristic of magnetobremsstrahlung of accelerated particles. We have found fluxes in four VUV ranges for a selected area (the region of emission of the PE arcade), and determined the amount of plasma with various temperatures. We have compared these quantities with RHESSI soft X-ray data, and used the corresponding information on the multi-temperature source to calculate the thermal radio emission. As an illustration, we have presented a simple case assuming that the magnetic field varies linearly with height. In a multi-temperature analysis, even such a model naturally yields a form for the radio spectrum similar to that observed with the RATAN-600. A more detailed model will be published in a future paper.

Thus, we confirm that the main effect in the decay stage of a flare is the formation of a large quantity of hot plasma that exists for many hours. The contribution of accelerated particles to the emission in the considered ranges is negligible for moderate- and low-power events. Only in the most powerful events can this contribution become appreciable, especially just after the formation of an arcade.

However, the model we have developed requires the presence of a magnetic field with an intensity of about 1000 G at the base of the tubes, at the photosphere level. Direct measurements have not indicated such field intensities in the small active-region elements accessible to present-day observations.

ACKNOWLEDGMENTS

The authors are grateful to the STEREO and RATAN-600 teams, as well as the GOES and SOHO staff, for the opportunity to work with these data. This work was supported by the Russian Foundation for Basic Research (project 11-02-00264) and the Basic Research Program of the Division of Physical Sciences of the Russian Academy of Sciences "Plasma Processes in the Solar System" (OFN-15).

REFERENCES

1. V. M. Grechnev, S. V. Kuzin, A. M. Urnov, et al., Solar Syst. Res. **40**, 286 (2006).
2. A. T. Altyntzev, V. V. Grechnev, H. Nakajima, et al., Astron. Astrophys. **113**, 415 (1999).
3. L. K. Harra-Murnion, B. Schmieder, L. van Driel-Gesztelyi, et al., Astron. Astrophys. **337**, 911 (1998).
4. S. Kamio, H. Kurokawa, and T. Ishi, Solar Phys. **215**, 127 (2003).
5. K. Ichimoto and T. Sakurai, The Flare Telescope and Norikura Team, in *Proceedings of the 2nd Japan–China Seminar on Solar Physics*, Ed. by T. Sakurai, T. Hirayama, and G. Ai (NAO, Tokyo, 1994), p. 151.
6. V. V. Grechnev, A. M. Uralov, I. A. Zandanov, et al., Publ. Astron. Soc. Jpn. **58**, 55 (2006).
7. V. N. Borovik, G. B. Gelfreikh, V. M. Bogod, et al., Solar Phys. **124**, 157 (1989).
8. I. Yu. Grigorieva, V. N. Borovik, M. A. Livshits, et al., Solar Phys. **260**, 157 (2009).
9. V. M. Bogod, A. M. Alesin, and A. A. Pervakov, Astrofiz. Byull. **66** (2011, in press).
10. M. J. Aschwanden, L. F. Burlaga, M. L. Kaiser, et al., Space Sci. Rev. **136**, 67 (2008).
11. M. J. Aschwanden, J. P. Wuesler, and N. V. Nitta, Solar Phys. **256**, 3 (2009).
12. A. M. Urnov, S. V. Shestov, S. A. Bogachev, et al., Astron. Lett. **33**, 396 (2007).
13. F. F. Goryaev, S. Parenti, A. M. Urnov, et al., Astron. Astrophys. **523**, A44 (2010).
14. V. V. Zheleznyakov, Sov. Astron. **7**, 630 (1963).
15. E. Ya. Zlotnik, Sov. Astron. **12**, 245 (1968).
16. E. Ya. Zlotnik, Sov. Astron. **12**, 464 (1968).
17. M. A. Livshits, V. N. Obridko, and S. B. Pikel'ner, Sov. Astron. **10**, 909 (1966).
18. E. Ya. Zlotnik, T. I. Kal'tman, and O. A. Sheiner, Astron. Lett. **33**, 168 (2007).
19. E. Ya. Zlotnik, T. I. Kal'man, and O. A. Sheiner, Astron. Lett. **33**, 371 (2007).
20. L. V. Yasnov, T. I. Kal'tman, and V. M. Bogod, Astron. Rep. **55**, 82 (2011).
21. Sh. B. Akhmedov, G. B. Gelfreikh, V. M. Bogod, and A. N. Korzhavin, Solar Phys. **79**, 41 (1982).

Translated by G. Rudnitskii